

Dual vortices and gauge choice in Abelian projected SU(2) lattice gauge theory

Kenneth Bernstein, Giuseppe Di Cecio and Richard W. Haymaker*

Department of Physics and Astronomy

Louisiana State University

Baton Rouge, Louisiana 70803 USA

Abstract

We explore vortex formation for Abelian projected SU(2) in the Polyakov gauge and compare the results with those calculated in the maximal Abelian gauge. In both gauges, a non-zero vacuum expectation value of a monopole field operator signals confinement. We find vortices in the Polyakov projection, confirming the connection between the dual superconductor order parameter and the existence of vortices. However we find that the Polyakov Abelian projection is problematic, leaving the maximal Abelian projection as the best candidate to define an effective theory of confinement in this scenario.

Typeset using REVTeX

*bernsten, dicecio and haymaker@rouge.phys.lsu.edu

I. INTRODUCTION

The key principle governing the onset of superconductivity is the spontaneous breaking of the U(1) gauge symmetry via a non-zero vacuum expectation value of a charged field [1]. An immediate consequence of this is the generation of a photon mass and, for type II superconductors, the formation of vortices which confine magnetic flux to narrow tubes as revealed by the Ginzburg-Landau theory [2–6]. Lattice studies of dual superconductivity in SU(N) gauge theories seek to exploit this connection in establishing the underlying principle governing color confinement.

On a four dimensional lattice, the effective Euclidean lattice Higgs theory is the appropriate generalization of the Ginzburg-Landau theory. The Higgs field is a 0-form living on the sites and the gauge field is a 1-form living on the links. Classical solutions to this theory exhibit the connection between the non-zero vacuum expectation value of the Higgs field and vortex formation.

In U(1) lattice pure gauge theory (no Higgs field), this same connection is seen to be present, not in the defining variables, but rather in the dual variables. More specifically:

1. A field with non-zero magnetic monopole charge, Φ , has been constructed [7–10]. It is a composite 4-form living on hypercubes constructed from gauge fields. There are also monopole current 3-forms.

On the dual lattice this monopole operator is a 0-form living on dual sites. The monopole currents are 1-forms living on dual links. These currents either form closed loops or end at monopole operators.

The monopole operator has a non-zero vacuum expectation value in the dual superconducting phase, $\langle \Phi \rangle \neq 0$, thereby signaling the spontaneous breaking of the U(1) gauge symmetry.

2. Dual Abrikosov vortices have been seen in simulations [11,12]. They are identified by the signature relationship between the electric field and the curl of the monopole

current in the transverse profile of the vortex. The dual coherence length, ξ_d measures the characteristic distance from a dual-normal-superconducting boundary over which the dual-superconductivity turns on. The dual London penetration length, λ_d measures the attenuation length of an external field penetrating the dual-superconductor. The dual photon mass $\sim 1/\lambda_d$ and the dual Higgs mass $\sim 1/\xi_d$.

A signal $\langle \Phi \rangle \neq 0$ without the consequent signal of a dual photon mass does not imply confinement. An observation of a dual photon mass, i.e. vortex formation, without $\langle \Phi \rangle \neq 0$ does not reveal the underlying principle governing the phenomenon.

The lattice Higgs theory, treated as an effective theory, i.e. limited to classical solutions, and considered in the dual sense, provides a model for interpreting simulations of the pure gauge theory that can reveal these important connections.

The link of these considerations to confinement in non-Abelian gauge theory is through the Abelian projection [13]. One first fixes the gauge while preserving U(1) gauge invariance. The non-Abelian gauge fields can be parametrized in terms of a U(1) gauge field and charged coset fields. The working hypothesis is that operators constructed from the U(1) gauge field alone, i.e. Abelian plaquettes, Abelian Wilson loops, Abelian Polyakov lines and monopole currents, will exhibit the correct large distance correlations relevant for confinement. But there is as yet no definitive way to choose the gauge which defines the Abelian projection and hence no unique way to define Abelian links and coset fields from the SU(2) links.

We are seeking a judicious choice of dynamical variables — defined by a particular Abelian projection — which can account for confinement via an effective theory involving these dynamical variables. This should be our first goal. If this is solved satisfactorily, then we can investigate how the picture changes if we go to an alternative set of variables — a different Abelian projection — since the phenomenon we are describing is of course gauge invariant. We do not expect that the same mechanism would describe confinement in two different Abelian projections.

There is a very nice illustration of this point in a paper by Chernodub, Polikarpov and

Veselov [14]. They compare two Abelian projections.

- The first is the maximal Abelian gauge [16] which is the most widely studied and perhaps the most promising candidate. Monopoles are the magnetic charge carriers of the persistent currents.
- Second they exhibit an Abelian projection in which confinement is due to objects other than monopoles. They choose the “minimal Abelian projection” and show that confinement is due to topological objects which are denoted “minipoles”.

Here we have two projections, two sets of dynamical variables, and two different descriptions of confinement, both viable candidate mechanisms.

Our goal in this paper is to test the connection between vortex formation and a non-zero vacuum expectation of the monopole field in the same Abelian projection. There is an intimate connection between these two results in a Higgs theory and hence it is a strong test of the idea for the dual theory. The two obvious candidate projections are the Polyakov gauge and the Maximal Abelian gauge.

Polyakov Gauge: Del Debbio, Di Giacomo, Paffuti and Pieri [17] have constructed a monopole field operator that shows a very strong signal with a sharp discontinuity in the vacuum expectation value of the monopole operator as a function of temperature in the neighborhood of T_c , the deconfining temperature. Their calculation is manifestly gauge invariant but a Polyakov line was used in the definition the monopole operator. In this sense we associate their calculation with the Polyakov gauge as we will explain further below. We look at vortex formation in the present paper.

Maximal Abelian gauge: The vortices are well established [12,18–21]. The static potential constructed from Abelian links gives as definitive a signal of confinement as the gauge invariant static potential as found by Suzuki et.al. [3,22], Stack et.al. [23,24] and Bali et. al. [25]. Bali et.al. find the Abelian string tension calculation gives

0.92(4) times the full string tension for $\beta = 2.5115$. Whether this approaches 1.0 in the continuum limit remains to be seen.

The calculation of Del Debbio et.al [17] of the monopole field operator as a practical matter is not adaptable to this gauge. It would require hundreds of gauge fixing sweeps of the whole lattice in order to accept or reject a single link update. Chernodub, Polikarpov and Veselov [26] have more recently calculated the constraint effective potential as a function of the monopole field in this gauge and found a symmetry breaking minimum. However they reported a problem of obtaining statistics and instead calculated an approximation to the effective potential.

In this paper we seek to establish vortex formation in the Polyakov gauge.

More recently Nakamura et al. [27] studied an alternative monopole operator defined in terms of the variables which occur in the monopole form of the action. We have not yet addressed the issue of establishing vortex formation in that framework.

We point out some technical difficulties in implementing the Polyakov Abelian projection. We use Abelian Polyakov lines to represent static sources. However they have an anomalous behavior which we discuss in Sec.IV. After an appropriate modification of the sources we find vortices. However they are suppressed relative to the analogous calculation in the Maximal Abelian gauge. Our conclusion is that the Polyakov Abelian projection is not likely to give a quantitative description of confinement within the confines of this particular scenario. The fact that there are vortices in conjunction with a non zero vacuum expectation value of a monopole operator confirms the connection we sought. However that is not enough to get agreement between the string tensions as this calculation shows. The charged coset fields are thought not to contribute to long range physics, but they are capable of partially screening the sources. This consideration does not arise in the U(1) theory because there is no charged dynamical field and this effect appears to be minimized in the maximal Abelian gauge.

We conclude in this paper that the screening due to these charged fields is quite large,

and that is why the vortices are suppressed. The signal of this suppression can be seen most easily in measurements of $divE$. Measuring this on a site coincident with the static source shows a very large attenuation in the Polyakov projection compared to the maximal Abelian projection. A recent measurement of a gauge invariant definition of $divE$ by Skala et. al. [28] for SU(3) which uses the Polyakov line to define the adjoint field exhibited no screening.

To unify the discussion of various choices of the Abelian projection in Sec. II we stress the introduction of a composite field $\hat{\phi}(x)$ constructed from the the gauge configuration $\{U_\mu(x)\}$. In Sec. III we review the gauge invariant definition of field strength in order to connect our calculation to the monopole operator calculation of Del Debbio et.al. [17] In Sec. IV we confront problems with the Polyakov gauge as mentioned above. We must represent static sources with Polyakov lines in order to study the theory at finite temperature. There is an inherent ambiguity on the lattice of ordering the eigenvalues of a diagonalized matrix at each site. The anomalous behavior is intimately connected with this freedom. We do not find a completely satisfactory solution, nevertheless we are led to an acceptable definition of sources. In Sec. V we present the results of our simulation.

II. DEFINITION OF THE COMPOSITE ADJOINT FIELD

The Abelian projection requires a gauge condition that breaks the SU(2) gauge invariance but preserves U(1) gauge invariance. This can be accomplished through the following two-step construction:

1. Consider a path ordered product of links, i.e. a Wilson line, which begins and ends at a particular site x . This defines an SU(2) group element, $W(x)$, e.g., an open plaquette or Polyakov line at the site x (no final trace at x). This in turn defines a composite field, $\phi(x)$.

$$W(x) = \cos \theta(x) + i\phi(x) \sin \theta(x), \quad \phi(x) = \hat{\phi}(x) \cdot \vec{\sigma}, \quad \hat{\phi}(x) \cdot \hat{\phi}(x) = 1, \quad \theta \in [0, \pi]. \quad (2.1)$$

This composite field transforms under the adjoint representation of SU(2),

$$\phi(x) \rightarrow \tilde{\phi}(x) = g(x)\phi(x)g^\dagger(x). \quad (2.2)$$

We require two further generalizations to cover the adjoint field definitions used in this paper. (i) In the SU(2) fundamental representation, a sum of group elements is, up to a normalization, also a group element. Hence we can also construct an adjoint field from a sum of the above defined Wilson lines. (ii) Further, the gauge invariant path ordered products of links can include the adjoint field itself, $\phi(x')$, at sites along the path. This leads to a self consistent definition of an adjoint field as, e.g., the case of the maximal Abelian gauge.

2. After constructing $\phi(x)$, we then perform a gauge transformation at each x that fixes the adjoint field $\hat{\phi}(x)$ in the 3 direction

$$\hat{\phi}(x) \rightarrow (0, 0, \pm 1), \quad \forall x. \quad (2.3)$$

This gauge fixing construction is invariant under subsequent U(1) gauge transformations which rotate in the (1, 2) plane, leaving the 3 direction invariant.

The ambiguity of rotating $\hat{\phi}(x)$ into the + or - 3-direction is equivalent to the choice of ordering the eigenvalues of $\hat{\phi}(x) \cdot \vec{\sigma}$. There are 2^N variants on gauge fixing corresponding to choosing +1 or -1 in the 3-direction at each of the N sites. We address this issue in Sec. IV.

A. Polyakov Gauge

The Polyakov gauge is defined by the above construction in which $W(x)$ is taken to be an open Polyakov line, $P(x)$ beginning and ending at x .

$$P(x) = \cos \theta(x) + i\phi_P(x) \sin \theta(x), \quad \phi_P(x) = \hat{\phi}_P(x) \cdot \vec{\sigma}, \quad \hat{\phi}_P(x) \cdot \hat{\phi}_P(x) = 1, \quad \theta \in [0, \pi]. \quad (2.4)$$

In Section IV we argue there that we should choose $\hat{\phi}_P(x) \rightarrow (0, 0, +1)$ at all sites, or equivalently $(0, 0, -1)$ at all sites.

B. Maximal Abelian gauge

1. Formulation in terms of an adjoint composite field

The maximal Abelian gauge [16] is conventionally defined as a configuration, $\{U_\mu(x)\}$, which maximizes $\mathcal{R}[U_\mu(x)]$,

$$\mathcal{R}[U_\mu(x)] = \sum_{x,\mu} \frac{1}{2} \text{Tr} \left[\sigma_3 U_\mu(x) \sigma_3 U_\mu^\dagger(x) \right], \quad (2.5)$$

over the set of gauge equivalent configurations $\{U_\mu(x)\}$. The continuum limit of this condition is

$$\left(\partial_\mu \pm igA_\mu^3 \right) \left[A_\mu^1 \pm iA_\mu^2 \right] = 0. \quad (2.6)$$

We wish to cast this into the language of the composite adjoint field. To do this let us consider a gauge fixing sweep in which we propose a gauge transformation on the links $U_\mu(x) \rightarrow U'_\mu(x) = g(x)U_\mu(x)g^\dagger(x+\mu)$ to test for an increase in \mathcal{R} . Then \mathcal{R} becomes

$$\begin{aligned} \mathcal{R}[U'_\mu(x)] &= \sum_{x,\mu} \frac{1}{2} \text{Tr} \left[\sigma_3 U'_\mu(x) \sigma_3 U'^\dagger_\mu(x) \right], \\ &= \sum_{x,\mu} \frac{1}{2} \text{Tr} \left[\sigma_3 \left(g(x)U_\mu(x)g^\dagger(x+\mu) \right) \sigma_3 \left(g(x+\mu)U^\dagger_\mu(x)g^\dagger(x) \right) \right], \\ &= \sum_{x,\mu} \frac{1}{2} \text{Tr} \left[\left(g^\dagger(x)\sigma_3 g(x) \right) U_\mu(x) \left(g^\dagger(x+\mu)\sigma_3 g(x+\mu) \right) U^\dagger_\mu(x) \right]. \end{aligned} \quad (2.7)$$

Hence a proposed gauge transformation of U is equivalent to proposing a change in the component of $\vec{\sigma}$ from σ_3 at each site to $\phi(x) = \hat{\phi}(x) \cdot \vec{\sigma}$, while leaving U unchanged.

Let us reformulate this procedure slightly by defining a gauge invariant quantity \mathcal{S} similar to \mathcal{R} but in which σ_3 is promoted to a variable $\phi(x) = \hat{\phi}(x) \cdot \vec{\sigma}$ transforming as Eqn.(2.2).

$$\mathcal{S}[\phi(x)] = \sum_{x,\mu} \frac{1}{2} \text{Tr} \left[\phi(x) U_\mu(x) \phi(x+\mu) U^\dagger_\mu(x) \right]. \quad (2.8)$$

We search for the maximum by proposing $\{\phi'(x)\}$, while holding $\{U_\mu(x)\}$ constant, to test for an increase in \mathcal{S} .

Having found the maximum, if we then perform a gauge transformation on both ϕ and U , which rotates $\hat{\phi}(x) \rightarrow (0, 0, +1)$, or $(0, 0, -1)$ for all x , then $\mathcal{S} \rightarrow \mathcal{R}$. But \mathcal{S} is gauge

invariant by construction and hence in this last step, the value of \mathcal{S} does not change, and the transformed links are the solution to the maximization problem, Eqn.(2.5).

This construction divides the maximal Abelian gauge fixing procedure into two logically independent steps described above, unifying maximal Abelian gauge fixing with other gauge fixing schemes.

2. Stationary condition

In order to find the set $\{\phi(x)\}$ corresponding to the maximum of \mathcal{S} , consider variations of \mathcal{S} about the stationary point under an infinitesimal transformation of $\phi(x)$, while leaving $\{U_\mu(x)\}$ constant:

$$\begin{aligned} \phi(x) &\rightarrow \tilde{\phi}(x) = \exp\{-i\vec{\eta}(x) \cdot \vec{\sigma}\} \phi(x) \exp\{+i\vec{\eta}(x) \cdot \vec{\sigma}\} \\ &= \left\{1 - i\vec{\eta}(x) \cdot \vec{\sigma} - \frac{1}{2}\eta^2(x)\right\} \phi(x) \left\{1 + i\vec{\eta}(x) \cdot \vec{\sigma} - \frac{1}{2}\eta^2(x)\right\}. \end{aligned} \quad (2.9)$$

The condition that \mathcal{S} is stationary under these variations is

$$\text{Tr}\left([\vec{\eta}(x) \cdot \vec{\sigma}, \phi(x)]\Phi(x)\right) = 0, \quad \forall x, \quad (2.10)$$

where $\Phi(x)$ is defined

$$\Phi(x) \equiv \sum_1^8 \phi(x)|_{p.t.} \quad (2.11)$$

The notation $|_{p.t.}$ means that the quantity is parallel transported to the point x as indicated in Fig. 1. The sum is over the nearest neighbor sites to the point x . Writing $\Phi(x) = \vec{\Phi}(x) \cdot \vec{\sigma}$, the stationary condition, Eqn. (2.10), gives:

$$\vec{\eta}(x) \cdot \hat{\phi}(x) \times \vec{\Phi}(x) = 0, \quad \forall x. \quad (2.12)$$

Since $\vec{\eta}(x)$ is arbitrary, $\hat{\phi}(x)$ must be either parallel or antiparallel to $\vec{\Phi}(x)$ at each site. Therefore

$$\epsilon(x)\hat{\phi}(x) = \frac{\vec{\Phi}(x)}{|\vec{\Phi}(x)|} = \hat{\Phi}(x), \quad \forall x, \quad (2.13)$$

where $\epsilon(x) = \pm 1$.

Let us now examine the second derivatives of \mathcal{S} about the stationary point. Define

$$\Delta\mathcal{S} = \mathcal{S}[\tilde{\phi}(x)] - \mathcal{S}[\phi(x)]. \quad (2.14)$$

Then, using the stationary condition, Eqn. (2.13), and keeping second order terms

$$\Delta\mathcal{S} \approx \frac{1}{2} \sum_x \left[-\eta^2(x) \frac{1}{2} Tr \left(\phi(x) \Phi(x) \right) + \frac{1}{2} Tr \left(\vec{\eta}(x) \cdot \vec{\sigma} \phi(x) \vec{\eta}(x) \cdot \vec{\sigma} \Phi(x) \right) \right]. \quad (2.15)$$

This can be cast into the form

$$\Delta\mathcal{S} \approx - \sum_x \epsilon(x) |\vec{\Phi}(x)| (\vec{\eta}(x) \times \hat{\phi}(x))^2. \quad (2.16)$$

This shows that the second derivative with respect to the variables $\{\eta(x)\}$ is $\epsilon(x) \times$ a negative number. If we choose $\epsilon(x) = +1$ for all x , then \mathcal{S} is a local maximum under these infinitesimal variations. This defines the composite adjoint field $\phi_{MA}(x)$, i.e. step (1) in the process.

In step (2) we perform a gauge transformation which takes $\hat{\phi}$ into the 3-direction. If we choose a gauge transformation that brings $\phi \rightarrow +\sigma_3$ at all sites, then \mathcal{S} is cast into the form \mathcal{R} . This is the transformation to the the maximal Abelian gauge, and justifies our notation: $\phi_{MA}(x)$. Equivalently, we can take $\phi \rightarrow -\sigma_3$ at all sites and reach the same conclusion.

Consider a solution corresponding to $\epsilon(x) = +1, \forall x$. If we then set $\epsilon(x') \rightarrow -1$ at one site, x' , and search anew for a solution, we will then obtain one in which $\hat{\phi}$ is given by the normalized average of $\hat{\phi}$ at the neighboring sites, parallel transported to x , except that $\hat{\phi}(x')$ is antiparallel to the average of its neighbors. Equation(2.16), shows that the new solution is no longer a local maximum of \mathcal{S} and hence it is not associated with the maximal Abelian gauge. We will return to this issue in a discussion of the minimal Abelian gauge in Sec. IV.

In order to find a stationary solution one can start with an arbitrary configuration $\{\phi(x)\}$ and then iterate. To update the site x , one calculates $\hat{\Phi}(x)$, Eqn.(2.11), based on the current neighboring ϕ 's. Then set

$$\left[\hat{\phi}(x) + \zeta (\hat{\Phi}(x) - \hat{\phi}(x)) \right]_{normalized} \rightarrow \hat{\phi}(x), \quad (2.17)$$

where ζ is the over-relaxation parameter. For $\zeta = 1$ we go directly to the stationary point for that site based on the current values of the neighboring $\hat{\phi}$'s. However by employing over-relaxation with $\zeta \approx 1.7$, the overall search rate for a self consistent solution is greatly enhanced. We tune this parameter to optimize performance.

This procedure requires an iterative search for a solution but it does not require iterative gauge transformations. After finding a solution, a single gauge transformation brings the gauge field into the maximal Abelian gauge. This method of obtaining the maximal Abelian gauge involves fewer multiplications than directly maximizing \mathcal{R} through gauge transformations and hence is a little faster.

The maximal Abelian gauge condition has multiple solutions, known as Gribov copies [29] for a given field configuration. The particular solution depends on the initial configuration and on the update algorithm. However Bali et. al. [25] have studied these multiple solutions and have offered an algorithm that limits this ambiguity. This Gribov ambiguity does not seem to have a large effect on the measured values of Abelian projected observables. In our discussion of the maximal Abelian gauge, we should understand that the above procedure is very unlikely to find the global maximum since there is no direct procedure to achieve that. Hence it must be understood that in general we are only at a local maximum, not the global maximum, of \mathcal{R} .

III. GAUGE INVARIANT DEFINITION OF ABELIAN FIELD STRENGTH

The lattice Georgi-Glashow model [30] has an elementary adjoint Higgs field living on the sites coupled to the gauge field living on the links. This allows one to define a gauge invariant field strength. The lattice definition of this is given in Fig. 2. This is the construction used to identify the ordinary magnetic field due to monopoles in non-Abelian gauge theory [31]. The classical continuum limit of these operators gives:

$$P_{\mu\nu} \approx -iga^2 Tr \left[\phi \left(\partial_\mu A_\nu - \partial_\nu A_\mu - ig[A_\mu, A_\nu] \right) \right]$$

$$+\frac{1}{2}a^2\text{Tr}\left[\phi\left(\partial_\mu\phi-ig[A_\mu,\phi]\right)\left(\partial_\nu\phi-ig[A_\nu,\phi]\right)\right], \quad (3.1)$$

where A_μ is defined $U_\mu = \exp(-igaA_\mu)$, a is the lattice spacing and g is the gauge coupling.

This manifestly gauge invariant form can be cast into the alternative form:

$$P_{\mu\nu} \approx -iga^2 F_{\mu\nu} = -iga^2 \left[\partial_\mu(\hat{\phi} \cdot \vec{A}_\nu) - \partial_\nu(\hat{\phi} \cdot \vec{A}_\mu) - \frac{1}{g} \hat{\phi} \cdot (\partial_\mu \hat{\phi}) \times (\partial_\nu \hat{\phi}) \right], \quad (3.2)$$

where we have used $\phi = \hat{\phi} \cdot \vec{\sigma}$, $(\hat{\phi} \cdot \hat{\phi} = 1)$, and $A_\mu = \vec{A}_\mu \cdot \vec{\sigma}/2$.

We can implement a gauge transformation that brings $\hat{\phi} \rightarrow (0, 0, 1)$ for all x . Then the last term of Eqn. (3.2) vanishes. The first term gives a conventional Abelian field strength,

$$F_{\mu\nu} = \partial_\mu W_\nu - \partial_\nu W_\mu; \quad W_\mu \equiv (\hat{\phi} \cdot \vec{A}_\mu) = (\vec{A}_\mu)_3. \quad (3.3)$$

Whether $\hat{\phi}$ denotes an elementary Higgs field, or a composite adjoint field as we discussed in Sec. II, this definition of field strength, Eqn. (3.1), is a manifestly gauge invariant quantity. However this is perhaps misleading in the composite adjoint field case because the definition of the field is identified with a specific gauge choice.

Del Debbio et al. [17] employed $\hat{\phi}_P$ in defining the Abelian field strength. This was needed in order to construct the monopole field operator. The vacuum expectation value of this field gave a very clear signal for dual superconductivity. Although their construction is manifestly gauge invariant, it is identified with the Polyakov gauge in the sense of this section. It is this connection that prompted us to study vortex formation in the Polyakov gauge to probe the connection between vortices and a non-zero vacuum expectation value.

IV. ADJOINT FIELD AND THE ABELIAN PROJECTION

The Abelian projection consists of (i) choosing a gauge that preserves a U(1) gauge invariance, and (ii) identifying Abelian links associated with that residual invariance [15]. In Sec. II we discussed the first step of choosing the gauge except for the ambiguity of transforming $\hat{\phi}$ into the +3 or -3-direction at each site. We will argue here that the +3-direction is the preferred choice for all sites or -3 for all sites. However this leads to an

unsettling result for the Polyakov gauge as we point out in part B below. Hence we are led to examine the issue more broadly to check out alternatives in the following parts of this section. There are 2^N choices, where N is the number of sites.

The choice of rotating $\hat{\phi}$ into the + 3-direction at every site is the prescription one would anticipate in order to get a smooth classical limit in which the changes in the gauge field are small between one site and its neighbors. But we feel alternatives should be presented for the record. The reader can skip to Part H, the conclusion for this section, without losing continuity. We have summarized the key results of this section in Table I.

A. Abelian links

For the purpose of defining Abelian links, consider the parametrization [14]:

$$U_\mu(x) = \begin{pmatrix} \cos(\phi_\mu(x))e^{i\theta_\mu(x)} & \sin(\phi_\mu(x))e^{i\chi_\mu(x)} \\ -\sin(\phi_\mu(x))e^{-i\chi_\mu(x)} & \cos(\phi_\mu(x))e^{-i\theta_\mu(x)} \end{pmatrix}, \quad (4.1)$$

$$\phi_\mu \in \left(0, \frac{\pi}{2}\right), \quad \theta_\mu, \chi_\mu \in (-\pi, \pi).$$

The Abelian link is defined through the factorization of Eqn. (4.1)

$$\begin{pmatrix} \cos(\phi_\mu(x)) & \sin(\phi_\mu(x))e^{i\gamma_\mu(x)} \\ -\sin(\phi_\mu(x))e^{-i\gamma_\mu(x)} & \cos(\phi_\mu(x)) \end{pmatrix} \begin{pmatrix} e^{i\theta_\mu(x)} & 0 \\ 0 & e^{-i\theta_\mu(x)} \end{pmatrix}, \quad (4.2)$$

where $\gamma_\mu(x) = \chi_\mu(x) + \theta_\mu(x)$. The Abelian link is given by $U_\mu(x) = e^{i\theta_\mu(x)}$. The complex coset field is given by $\sin(\phi_\mu(x))e^{i\gamma_\mu(x)}$. Under a U(1) gauge transformation, $g(x) = e^{i\alpha(x)\sigma_3}$

$$\theta_\mu(x) \rightarrow \theta_\mu(x) + \alpha(x) - \alpha(x + \mu), \quad (4.3)$$

$$\gamma_\mu(x) \rightarrow \gamma_\mu(x) + 2\alpha(x).$$

The coset vector fields live on the sites and are doubly charged.

The ambiguity of rotating $\widehat{\phi}$ to the ± 3 direction, $\phi = \pm\sigma_3$, is the same as the ambiguity of ordering the eigenvalues of this 2×2 diagonal matrix. The order of the eigenvalues for a particular link can be interchanged via an $SU(2)$ gauge transformation $g = i\sigma_2$ at the two neighboring sites corresponding to the link in question.

B. The Polyakov gauge with the + prescription

Translation invariance suggests that whatever rule we adopt for ordering the eigenvalues, we should use the same rule at every site. Let us choose $\phi = +\sigma_3$, denoting this as the + prescription.

In the Polyakov gauge if we choose $\phi_P = +\sigma_3$ at every site, then there is a difficulty. The $SU(2)$ Polyakov line, Eqn. (2.1), can be written

$$\begin{pmatrix} e^{i\theta_P(x)} & 0 \\ 0 & e^{-i\theta_P(x)} \end{pmatrix}, \quad \theta_P(x) \in [0, \pi]. \quad (4.4)$$

The 11 element of this is the $U(1)$ Polyakov line $P(x) = e^{i\theta_P(x)}$. Since θ_P is distributed in the domain $[0, \pi]$ the imaginary part of $P(x)$ can not be negative. As a consequence, the average of $P(x)$ will have a non-zero imaginary part due to this kinematical effect. This is anomalous. Polyakov lines represent static sources. If we are to get the ‘expected’ distribution in which θ is distributed symmetrically in the domain $(-\pi, \pi]$ we would need a rule that allows the choice $\phi_P = -\sigma_3$ with a statistical weight equal to the $\phi_P = +\sigma_3$ case.

If we choose $\phi \rightarrow -\sigma_3$ at all sites, we reach the same conclusion except that $Im(P(x))$ can not be positive.

C. U(1) gauge theory as a guide

We can examine the $U(1)$ model for guidance. We expect Abelian projected $SU(2)$ to resemble the $U(1)$ theory. Consider the limit in which the $SU(2)$ theory goes over to the $U(1)$

theory. In $SU(2)$ the links lie in the group manifold S_3 . In $U(1)$ they lie in a submanifold S_1 . Consider adding a term to the action that is invariant under $U(1)$ but which breaks $SU(2)$. Further choose it to bias the links into a peaked distribution centered on S_1 . Then as the width of the peak approaches zero, the $SU(2)$ theory goes over to the $U(1)$ theory. In $U(1)$, the Polyakov line $P(x) = e^{i\theta_P(x)}$ takes values for θ_P distributed in the domain $(-\pi, \pi]$. Positive and negative values of θ_P are equally probable.

D. The \pm prescription \iff random prescription

To try to resolve the discrepancy between the $U(1)$ theory and Abelian projected $SU(2)$ in the $+$ prescription, let us consider a prescription in which we choose $+$ or $-$ depending on the value of $\hat{\phi}(x)$. For example, we can correlate the signs $+$ or $-$ with the sign of $[\hat{\phi}(x)]_3$. In other words, if $\hat{\phi}(x)$ is in the upper hemisphere then choose $+$. If it is in the lower hemisphere then choose $-$. We denote this the \pm prescription. The phase of the Abelian Polyakov line will now be distributed in the expected way, $(-\pi, \pi]$. This is perhaps the prescription most closely associated with the limiting procedure in the previous section.

This prescription is equivalent to choosing $+$ or $-$ randomly. The reason is that a gauge transformation can give an arbitrary orientation to $\hat{\phi}$. If after each update, we follow it with a random gauge transformation, (an update followed by a gauge transformation is indistinguishable from an update alone) then the assignments of $+$ or $-$ at each site will be random. The $SU(2)$ transformations do not respect the homotopy classes of $U(1)$.

E. The Polyakov gauge with the \pm prescription

We now apply the \pm prescription to the Abelian projection in the Polyakov gauge and point out a flaw in this choice.

Let P denote the open Polyakov line at site x , and P' the open Polyakov line at the neighboring site in the $+x_4$ direction. Then

$$PU = UP', \quad (4.5)$$

where U is the link in the x_4 direction connecting the two sites.

Now go to the Polyakov gauge. Suppose we choose $\phi_P = +\sigma_3$ at both sites. Then $P = P'$ and the solution to Eqn. (4.5) gives

$$U = u_4 + iu_3\sigma_3, \quad u_3^2 + u_4^2 = 1, \quad (4.6)$$

showing that the links in the x_4 direction are diagonal. Contrast this with the case in which we choose $\phi_P = +\sigma_3$ at one site and $\phi_P = -\sigma_3$ at the neighboring site. Then $P' = P^\dagger$ and the solution to Eqn. (4.5) gives

$$U = i(u_1\sigma_1 + u_2\sigma_2) \quad u_1^2 + u_2^2 = 1. \quad (4.7)$$

This second case does not give an acceptable Abelian projection since the x_4 Abelian link is undefined, i.e. the 11 element of the link matrix is zero.

We can still define a \pm prescription appropriately modified for the Polyakov gauge in which the spatial sites have independent random \pm choices, but that the choice is independent of the values of x_4 .

However this construction has a further problem. Consider the correlator shown in Fig. 3. *The correlation of the field strength with a product of two Abelian Polyakov lines representing a static quark-antiquark pair vanishes.* This correlation is given by

$$\langle e^{i(\pm\theta_P(x_1) \pm \theta_P(x_3))} \times \sin \theta_F(x_2) \rangle. \quad (4.8)$$

The \pm signs, arising from the prescription of a random gauge transformation, $g = i\sigma_2$, have the effect of flipping the sign of the charge of the two sources. With a statistical weight equal for each of the four signs, the field averages to zero.

The correlation also vanishes if one only considers random $i\sigma_2$ gauge transformation at the sites contiguous with the plaquette. Consider the parametrization of a link in Eqn. (4.1). We adopt this parametrization for a link in which the $+$ prescription is applied at both ends. The SU(2) link and the corresponding Abelian link are

$$U_\mu^{++} = \begin{pmatrix} \cos \phi_\mu e^{i\theta_\mu} & \sin \phi_\mu e^{i\chi_\mu} \\ -\sin \phi_\mu e^{-i\chi_\mu} & \cos \phi_\mu e^{-i\theta_\mu} \end{pmatrix}, \quad U_\mu^{Abelian} = e^{i\theta_\mu}. \quad (4.9)$$

Different prescriptions will change the SU(2) links and accordingly the choice of the Abelian angles. Let $i\sigma_2$ be the gauge transformation changing the orientation of the adjoint field. (This gauge transformation is defined up to a $U(1)$ transformation.) The link will transform according to one of the following cases:

$$U_\mu^{+-} = U_\mu^{++}(-i\sigma_2) = \begin{pmatrix} \sin \phi_\mu e^{i\chi_\mu} & -\cos \phi_\mu e^{i\theta_\mu} \\ \cos \phi_\mu e^{-i\theta_\mu} & \sin \phi_\mu e^{-i\chi_\mu} \end{pmatrix}, \quad U_\mu^{Abelian} = e^{i\chi_\mu}, \quad (4.10)$$

$$U_\mu^{-+} = i\sigma_2 U_\mu^{++} = \begin{pmatrix} -\sin \phi_\mu e^{-i\chi_\mu} & \cos \phi_\mu e^{-i\theta_\mu} \\ -\cos \phi_\mu e^{i\theta_\mu} & -\sin \phi_\mu e^{i\chi_\mu} \end{pmatrix}, \quad U_\mu^{Abelian} = e^{i(\pi - \chi_\mu)}, \quad (4.11)$$

$$U_\mu^{--} = i\sigma_2 U_\mu^{++}(-i\sigma_2) = \begin{pmatrix} \cos \phi_\mu e^{-i\theta_\mu} & \sin \phi_\mu e^{-i\chi_\mu} \\ -\sin \phi_\mu e^{i\chi_\mu} & \cos \phi_\mu e^{i\theta_\mu} \end{pmatrix}, \quad U_\mu^{Abelian} = e^{-i\theta_\mu} \quad (4.12)$$

where the $\pm\pm$ notation refers to the prescription at each end of the link.

After a random gauge transformation the *sin* of the Abelian plaquette angle will assume one of the forms shown in Fig. 4. We are working in the Polyakov gauge hence there are only four possibilities since the adjoint field must be constant in x_4 . All the above configurations have the same statistical weight and for each configuration there is always another configuration differing only by the sign. Hence the field strength in the presence of two sources vanishes in the \pm prescription according to this argument also.

This argument generalizes to any Wilson loop since the parametrization could apply to a Wilson line instead of a single link. Further we can replace the Polyakov line source by another Wilson loop and then we obtain

$$\langle \sin \theta_{W_1} \sin \theta_{W_2} \rangle = 0, \quad (4.13)$$

for the \pm prescription if the two Wilson loops do not share any spatial sites.

F. Gauge invariant field strength and the + prescription

To get further support for the + prescription consider the Abelian projected theory in the Polyakov gauge but instead of calculating the field strength from the Abelian plaquette let us instead represent the field strength by the manifestly gauge invariant form, Fig. 2.

In the Polyakov gauge, $\hat{\phi}(x)$ is independent of x_4 and as a consequence, the second term in Fig. 2 vanishes. Consider a static source represented by an Abelian Polyakov line at point x , and the field strength at point y as shown in Fig. 5(a).

Let us define variables for the (open) plaquette in Fig. 5(a) by

$$\cos \theta_F(y) + i\vec{\sigma} \cdot \hat{\phi}_F(y) \sin \theta_F(y). \quad (4.14)$$

Then the correlator is given by

$$\frac{\langle \sin \theta_P(x) \hat{\phi}_P(y) \cdot \hat{\phi}_F(y) \sin \theta_F(y) \rangle}{\langle \cos \theta_P \rangle} = \frac{\langle \sin \theta_P(x) (\hat{\phi}_F(y))_3 \sin \theta_F(y) \rangle}{\langle \cos \theta_P \rangle}, \quad (4.15)$$

where the last equality is due to the choice of the Polyakov gauge. Measuring the field strength with the Abelian plaquette, Fig. 5(b), gives

$$\frac{\langle \sin \theta_P(x) \sin \theta_F^{(Abelian)}(y) \rangle}{\langle \cos \theta_P \rangle}. \quad (4.16)$$

The field strength in Eqn. (4.15) is manifestly gauge invariant, and therefore the prescription at the site y has no bearing on the definition of the correlator. If we use the Abelian plaquette, Eqn. (4.16), instead, then the value depends on the prescription. However the + prescription has the same classical limit for small lattice spacing a as the classical limit of the gauge invariant form, Eqn.(3.3). This follows from the discussion in Sec. IV E. In Fig. 4 in the cases in which the four points of the plaquette have the same prescription, the Abelian plaquette has the standard classical limit. In the other cases, the plaquette involves angles arising from the off-diagonal elements of the SU(2) link.

For completeness we compare this to the connected definition of field strength at point y as shown in Fig. 5(c). In our notation the correlator is given by

$$\frac{\langle (\sin \theta_P(x) \widehat{\phi}_P(x))|_{p.t.(x \rightarrow y)} \cdot \widehat{\phi}_F(y) \sin \theta_F(y) \rangle}{\langle \cos \theta_P(x) \rangle}, \quad (4.17)$$

where $|_{p.t.(x \rightarrow y)}$ means that the variables are parallel transported from x to y in the same sense as applied to Eqn.(2.11).

G. Minimal Abelian projection

We consider only lattices which allow an even-odd checkerboard assignment to the sites. Consider two solutions of Eqn. (2.13), corresponding to different values of $\epsilon(x)$.

$$\begin{aligned} \widehat{\phi}_{MA}(x) : \quad \epsilon(x) &= +1 \quad \forall x, \\ \widehat{\phi}_{mA}(x) : \quad \epsilon(x) &= -1 \quad \forall x. \end{aligned} \quad (4.18)$$

For the case in which the LHS of Eqn. (2.13) involves only odd (even) sites then the RHS involves only even (odd) sites, and vice versa. Hence

$$\begin{aligned} \widehat{\phi}_{mA}(x) &= +\widehat{\phi}_{MA}(x), \quad x \text{ odd}(even), \\ &= -\widehat{\phi}_{MA}(x), \quad x \text{ even}(odd). \end{aligned} \quad (4.19)$$

In other words, the $\widehat{\phi}_{mA}(x)$ solution is identical to the $\widehat{\phi}_{MA}(x)$ solution except that it is flipped at the even (odd) sites. This is in contrast to the example in Sec. IIB where a change in $\epsilon(x)$ led to a new solution which has no simple relation to the old solution. We further note that each term in $\mathcal{S}[\phi(x)]$, Eqn.(2.8), involves $\widehat{\phi}(x)$ at an even site and $\widehat{\phi}(x)$ at an odd site. Therefore the effect of the flipping is to change the sign of \mathcal{S}

$$\mathcal{S}[\widehat{\phi}_{mA}] = -\mathcal{S}[\widehat{\phi}_{MA}] \quad (4.20)$$

Since $\widehat{\phi}_{MA}$ maximizes \mathcal{S} , it follows that $\widehat{\phi}_{mA}$ minimizes \mathcal{S} . This is corroborated by the stability analysis, Eqn.(2.16).

The adjoint field $\widehat{\phi}_{mA}$ defines the minimal Abelian projection introduced by Chernodub, Polikarpov and Veselov [14]. They showed that confinement is due to objects other than monopoles, which they denoted as minopoles.

H. Conclusion about the prescriptions

The arguments in this section lead us to adopt the + prescription for Abelian projected SU(2) in the Polyakov gauge. This prescription is not completely satisfactory. It does not go over smoothly to a U(1) theory as one might expect. This is indicated by the behavior of the phase angle of the Abelian projected Polyakov line. It is bounded 'artificially' in the interval $[0, \pi]$ giving the expectation value of the Polyakov line an anomalous imaginary part. The adjoint field defined for the maximal Abelian gauge is a construct that does relate directly to an observable in this sense and does not seem to cause a similar difficulty.

Further we must rethink how to represent static sources. The distribution of the Abelian Polyakov phase angle in the domain $[0, \pi]$ is weighted by the Haar measure, $\sin^2 \theta$ which is peaked at $\pi/2$. This means, e.g. that the average of two Polyakov lines

$$P_1 P_2^* = e^{i(\theta_1 - \theta_2)}, \tag{4.21}$$

will have a non-vanishing real part arising from the same kinematic effect. Our solution to this is to define the quark-antiquark source as the connected part of the product of the two Polyakov loops,

$$\langle P_1 P_2^* \rangle - \langle P_1 \rangle \langle P_2^* \rangle. \tag{4.22}$$

V. DUAL VORTICES AND ABELIAN PROJECTIONS

A. Measurements

In this section we study the electric flux and the magnetic monopole current distributions around static sources in the Polyakov gauge with the + prescription and the definition

of Abelian static sources as in Sec. IV H. Moreover we make a comparison between this projection and the maximal Abelian projection in which the main properties of dual vortices have already been studied.

Our simulations were performed on a $12^3 \times 4$ lattice with the standard form of the Wilson action. The calculation follows the method given in [18]. We used two Abelian Polyakov lines correlated along the 3-direction as static sources in the finite temperature theory. The longitudinal electric field between two charges separated by a distance d in the 3-direction is given by:

$$\langle E_z(x) \rangle = \frac{\langle P(0)P^\dagger(d) \sin \theta_{34}(x) \rangle}{a^2 e \langle P(0)P^\dagger(d) \rangle} = \frac{\langle \sin \theta_{PP^\dagger} \sin \theta_{34}(x) \rangle}{a^2 e \langle \cos \theta_{PP^\dagger} \rangle} \quad (5.1)$$

where θ_{34} is the angle of the Abelian plaquette in the 3 – 4 plane, θ_{PP^\dagger} is the angle of the product of the two Abelian Polyakov lines and e is the electric charge.

Magnetic monopole currents can be identified by the dual Maxwell equations that in the continuum are:

$$J_\mu^m = -\frac{1}{2} \epsilon_{\mu\nu\rho\sigma} \partial_\nu F_{\rho\sigma} \quad (5.2)$$

On the lattice one can choose [32]:

$$a^2 e F_{\mu\nu} = \sin \theta_{\mu\nu} \quad (5.3)$$

We measured the magnetic current distribution around static sources:

$$\langle (\text{curl} \vec{J}^m(x))_z \rangle = \frac{2\pi \langle \sin \theta_{PP^\dagger} (\text{curl} \vec{J}^m(x))_z \rangle}{a^4 e \langle \cos \theta_{PP^\dagger} \rangle} \quad (5.4)$$

where the curl of the magnetic current is constructed as in [18], and $2\pi/e$ is the magnetic charge.

B. Numerical results and discussion

We made our simulations at $\beta = 2.25$ and $\beta = 2.40$. As we chose the temporal extent of the lattice equal to 4, the first value of β corresponds to the confined phase while the second corresponds to the unconfined phase.

The results for the Polyakov gauge are shown in Fig. 6 for $d = 1a, 2a, 3a$. For $\beta = 2.25$ we see a clear signal for both the electric field and the curl of the magnetic currents on the axis of the two charges. As we move in the transverse direction r , we observe a rapid fall off of the electric field that always vanishes after a few lattice spacings and a behavior of the monopole current consistent with the predictions of the Ginzburg-Landau theory. As the distance d of the static charges increases, the values of the electric field decreases as expected.

In the unconfined phase ($\beta = 2.40$) we see a remarkably different behavior of the curl of the magnetic currents that is much smaller than in the other phase and at $d = 3a$ is consistent with zero everywhere. Moreover the electric field approaches zero less rapidly although not clearly evident from the figure.

A similar scenario has been found for the maximal Abelian gauge [18]. In Fig. 7 we show the results in this gauge for the case $d = 3a$. We used the procedure described in Sec. II to define the Abelian projection.

Although both Abelian projections produce results consistent with the Ginzburg-Landau theory, the dual superconductivity parameters are quite different for the two projections. We are not able to perform a quantitative analysis in order to evaluate the coherence length ξ_d and the London penetration length λ_d . Nevertheless while the data for the maximal Abelian gauge support a non-vanishing value for the coherence length, there is no evidence for ξ_d being different from zero in the Polyakov gauge.

Moreover a comparison between the two different projections shows that in the Polyakov gauge the peak values of the electric field and of the curl of the magnetic currents are more than an order of magnitude smaller than the correspondent values in the maximal Abelian gauge. Suzuki et. al. [33] reported similarly that the string tension was suppressed in the Polyakov gauge.

To understand these differences we remember that after Abelian projection we are left not only with the Abelian links but also with the coset vector fields. The dynamics of these doubly charged fields is clearly dependent on the choice of the Abelian projection. To show

the different role of the coset fields in the two projections, we measure the divergence of the electric field giving the spatial distribution of the electric charge. The divergence at site x is defined as

$$\langle \text{div} \vec{E}(x) \rangle = \sum_{i=1}^3 \frac{\langle \sin \theta_{PP^\dagger} (\sin \theta_{i4}(x) - \sin \theta_{i4}(x-i)) \rangle}{a^3 e \langle \cos \theta_{PP^\dagger} \rangle} \quad (5.5)$$

so that all the six plaquettes have in common the link starting at x and extending in the time direction. In Fig. 8 we show the results for two Polyakov lines separated by three lattice spacings. The figure clearly shows that the effective charge of the static source is much smaller in the Polyakov gauge and that the coset fields in the two prescriptions respond in opposite ways to the presence of an electric charge with the fields in the Polyakov gauge shielding the static charge. Skala et al. have studied $\text{div} \vec{E}$ in $SU(3)$ in a gauge invariant formulation and conclude there is no screening [28].

VI. CONCLUSIONS

Using the $U(1)$ theory as a guide, we explore the connection between (i) the non-vanishing of a vacuum expectation value of the monopole field and (ii) vortex formation. Item (i) provides the underlying principle, item (ii) gives direct evidence of a photon mass and confinement. In the Abelian projection of $SU(2) \rightarrow U(1)$ there is an additional consideration. After identifying the $U(1)$ gauge field, there remain dynamical charged vector coset fields. They can screen the static sources and change the electric flux, affecting the string tension.

From prior work we know that, e.g., the minimal Abelian projection and the maximal Abelian projection account for the physics of confinement through very different mechanisms. We anticipated that the monopoles in the Polyakov projection would give a picture very similar to the maximal Abelian gauge. However we found that the coset fields greatly suppress the static sources. It could be that we are much farther from the continuum limit than we thought. But that seems unlikely since other quantities are close to scaling values. Our definitions of field strength, monopoles, static sources etc. have some leeway, but all

should give the same continuum limit. Or it could be that the dynamical variables arising from the Polyakov Abelian projection do not adequately separate the short distance and long distance physics. This leaves the maximal Abelian gauge as the prime candidate to define an effective theory of confinement in this scenario.

ACKNOWLEDGMENTS

We would like to thank Adriano Di Giacomo and Tsuneo Suzuki for discussions. Work was partially supported by the Department of Energy under Grant No. DE-FG05-91ER40617. Giuseppe Di Cecio was partially supported by a University of Pisa postdoctoral fellowship.

REFERENCES

- [1] S. Weinberg, The Quantum Theory of Fields Vol II, Cambridge University Press, Cambridge 1996, See chapter 21.6 for a thorough treatment of this viewpoint.
- [2] For a review and further references see e.g. R.W. Haymaker, “*Dual Abrikosov vortices in $U(1)$ and $SU(2)$ lattice gauge theories*”, Proceedings of the international School of Physics “Enrico Fermi”, Course CXXX, A. Di Giacomo and D. Diakonov (Eds.) IOS Press, Amsterdam 1996, hep-lat 9510035.
- [3] For a review of monopoles and confinement, see e.g. T. Suzuki, Nucl.Phys. **B** Proc. Suppl. **30**, 176 (1993).
- [4] V. L. Ginzburg and L. D. Landau, Zh. Ekxperim, i Theor. Fiz, **20**, 1064 (1950).
- [5] A. A. Abrikosov, Sov. Phys. JETP **32**, 1442 (1957).
- [6] M. Tinkham, Introduction to Superconductivity, (McGraw-Hill, New York, 1975)
- [7] J. Frölich and P. A. Marchetti, Euro. Phys. Lett. **2**, 933 (1986); Commun. Math. Phys. **112**, 343 (1987); **116**, 127 (1988); **121**, 177 (1989); Lett. Math. Phys **16**, 347 (1988).
- [8] L. Polley and U.-J. Wiese, Nucl. Phys. **B356**, 621 (1991).
- [9] M. I. Polikarpov, L. Polley and U.-J. Weise, Phys. Lett. **B253**, 212 (1991).
- [10] L. Del Debbio, A. Di Giacomo and G. Paffuti, Phys. Lett. **B349**, 513, (1995); Nucl. Phys B (Proc. Suppl.) **42**, 231 (1995);
- [11] V. Singh, R.W. Haymaker, and D.A. Browne, Phys. Rev. **D47**, 1715 (1993).
- [12] R.W. Haymaker, V. Singh, D. Browne and J. Wosiek; Proc. of Workshop on QCD Vacuum Structure and its applications, The American University of Paris, June 1-5, 1992, p184, World Scientific 1993.
- [13] G. 't Hooft, Nucl. Phys. **B 190**, 455 (1981).

- [14] M.N. Chernodub, M.I. Polikarpov and A.I. Veselov, Phys. Lett. **B 342**, 303 (1995).
- [15] A.S. Kronfeld, G. Schierholz and U.J. Wiese, Nucl. Phys. **B 293**, 461 (1987);
- [16] A.S. Kronfeld, M.L. Laursen, G. Schierholz and U.J. Wiese, Phys. Lett. **B 198**, 516 (1987); T. Suzuki and I. Yotsuyanagi, Phys. Rev. **D 42**, 4257 (1990).
- [17] L. Del Debbio, A. Di Giacomo, G. Paffuti and P. Pieri, Phys. Lett. **B 355**, 255 (1995).
- [18] V. Singh, D.A. Browne, and R.W. Haymaker, Nucl. Phys. B (Proc. Suppl.) **30**, 658 (1993); Phys. Lett. **B306**, 115 (1993).
- [19] Y. Matsubara, S. Ejiri, and T. Suzuki, Nucl. Phys. **B34** (Proc. Suppl.) 176 (1994).
- [20] Y. Peng and R.W. Haymaker, Phys. Rev. **D 52** 3030, (1995).
- [21] P. Cea and L. Cosmai, Nucl. Phys. **B Proc. Suppl. 30**, 572 (1993); Phys. Rev. **D 52**, 5152 (1995).
- [22] H. Shiba and T. Suzuki, Phys. Lett. **B 333**, 461 (1994).
- [23] J. Stack and R. Wensley, Nucl. Phys. **D 22**, 597 (1992).
- [24] J. Stack, S. Neiman and R. Wensley, Phys. Rev. **D 50**, 3399 (1994)
- [25] G. S. Bali, V. Bornyakov, M. Müller-Preussker and K. Schilling, Phys. Rev. **D 54** 2863 (1996).
- [26] M.N. Chernodub, M.I. Polikarpov and A.I. Veselov, Nucl. Phys. Proc. Suppl. **49**, 307, (1996).
- [27] N. Nakamura, V. Bornyakov, S. Ejiri, S. Kitahara, Y. Matsubara and T. Suzuki, Lattice-96 conference abstract, St. Louis, June 1996 e-print 9608004.
- [28] P. Skala, M. Faber and M. Zach, Ahrenshoop Symp. 301-306, 1995 hep-lat/9603009.
- [29] V.N. Gribov, Nucl. Phys. **B 139**, 1 (1978).

- [30] H. Georgi and S.L. Glashow, Phys. Rev. Lett. **28**, 1494 (1972).
- [31] G. 't Hooft, Nucl. Phys. **B 79**, 276 (1974).
- [32] M. Zach, M. Faber, W. Kainz and P. Skala, Phys. Lett. **B 358**, 325 (1995).
- [33] T. Suzuki, S. Ilyar, Y. Matsubara, T. Okude and K. Yotsuji, Phys. Lett. **B 347**, 375 (1995); *ERRATUM-ibid.* **B 351**, 603 (1995).

FIGURES

FIG. 1. Parallel transport of adjoint field. The lines represent single links, U . The adjoint field, indicated by the circle, is normalized: $\phi^2 = I$, $\phi = \hat{\phi} \cdot \vec{\sigma}$.

FIG. 2. Definition of gauge invariant Abelian field strength. The lines represent single links, U . The adjoint field, indicated by the circle, is normalized: $\phi^2 = I$, $\phi = \hat{\phi} \cdot \vec{\sigma}$.

FIG. 3. Vanishing of the field strength in the presence of Polyakov lines.

FIG. 4. Cancellation of terms for the field strength in the \pm prescription.

FIG. 5. Correlators for measuring field strength in the neighborhood of a static source. (a) The form using the gauge invariant field strength, (b) using the Abelian plaquette, and (c) the connected correlator.

FIG. 6. Electric field and curl of monopole currents as a function of the transverse distance r from the axis of two static sources for the Polyakov gauge. For separation $d = 3a$ the signal in the region midway between the charges is drowned out by the noise, therefore we only show the result for the region close to one of the charges ($z=0$).

FIG. 7. Electric field and curl of magnetic currents as a function of r for the maximal Abelian gauge.

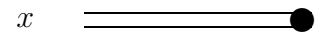
FIG. 8. Divergence of the electric field along the axis connecting two static charges separated by three lattice spacings.

TABLES

Gauge	P	Definition	Comments
Condition			
	“+” :		
		$\widehat{\phi}(x) \rightarrow (0, 0, +1), \forall x;$	
	“-” :		
		$\widehat{\phi}(x) \rightarrow (0, 0, -1), \forall x;$	
	“±”:		
		$\widehat{\phi}(x) \rightarrow (0, 0, \text{sgn}\{\widehat{\phi}(x)_3\});$	
	“random”:		
		$\widehat{\phi}(x) \rightarrow (0, 0, \text{random} \pm 1).$	
Polyakov	“+” or “-”	$P(x) = \cos \theta +$ $i\widehat{\phi}_P(x) \cdot \vec{\sigma} \sin \theta(x),$ Eqn.(2.4).	Im[Abelian Polyakov line] $\neq 0$. Classical limit of field strength same as classical limit of gauge invariant field strength.
	“±” ¹		Im[Abelian Polyakov line] = 0. Correlations vanish. Time-like Abelian links undefined. ¹
	“random” ¹		Equivalent to “±”. ¹
Maximal	“+” or “-”	$\widehat{\phi}_{MA}(x) = +\widehat{\Phi}_{MA}(x), \forall x,$	Maximizes $\mathcal{R}, \mathcal{S},$
Abelian		Eqn.(2.13), $\epsilon(x) = +1.$	Eqns.(2.5), (2.8).
Minimal	“+” or “-”	$\widehat{\phi}_{mA}(x) = -\widehat{\Phi}_{mA}(x), \forall x,$	Minimizes $\mathcal{R}, \mathcal{S},$
Abelian		Eqn.(2.13), $\epsilon(x) = +1.$	Eqns.(2.5), (2.8).

TABLE I. Summary of gauge fixing. (1. The problem in defining time-like Abelian links can be remedied by choosing either “+” or “-” at all sites along a particular Polyakov line.)

$$\phi(x)|_{p.t.} = U_\mu(x)\phi(x + \mu)U_\mu^\dagger(x)$$



$$\phi(x)|_{p.t.} = U_\mu^\dagger(x - \mu)\phi(x - \mu)U_\mu(x - \mu)$$

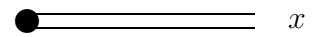


FIG. 1

$$P_{\mu\nu} = \text{[square diagram with dot at bottom-left]} + \frac{1}{2} \text{[L-shaped diagram with dots at top, bottom-left, and bottom-right]}$$

FIG. 2

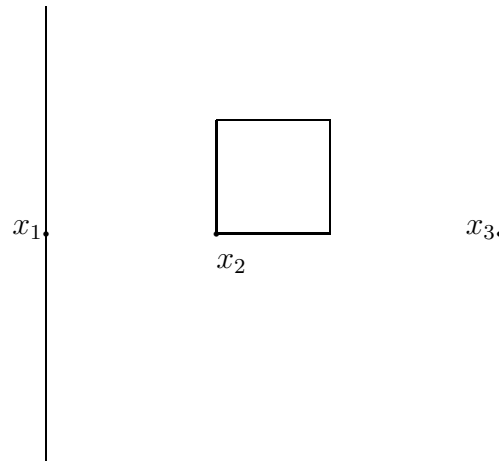
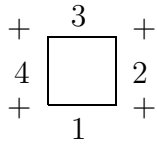
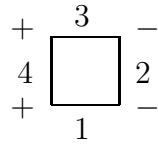


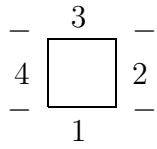
FIG. 3



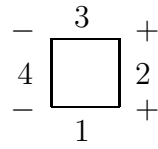
$$\sin(\theta_1 + \theta_2 - \theta_3 - \theta_4)$$



$$\sin(\chi_1 - \theta_2 - \chi_3 - \theta_4)$$



$$-\sin(\theta_1 + \theta_2 - \theta_3 - \theta_4)$$



$$-\sin(\chi_1 - \theta_2 - \chi_3 - \theta_4)$$

FIG. 4

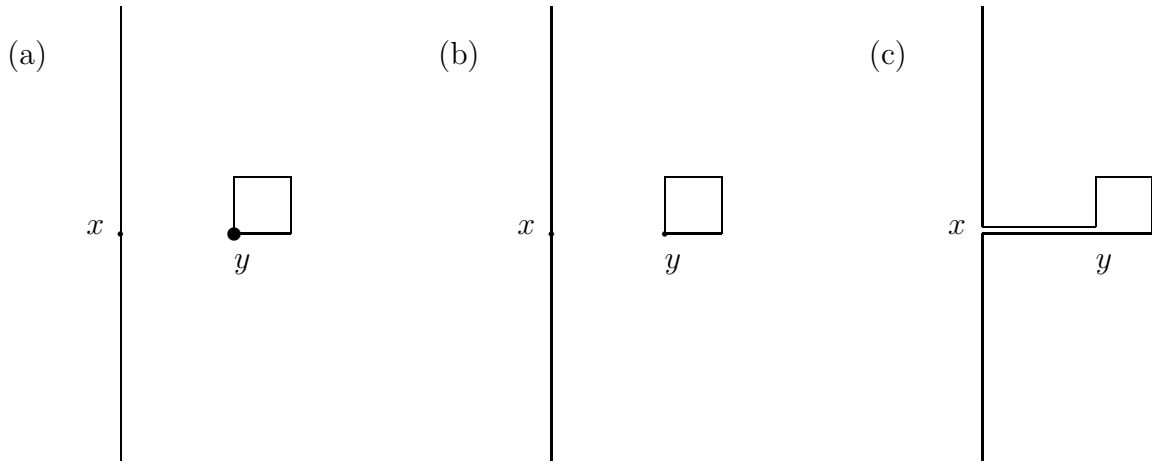


FIG. 5

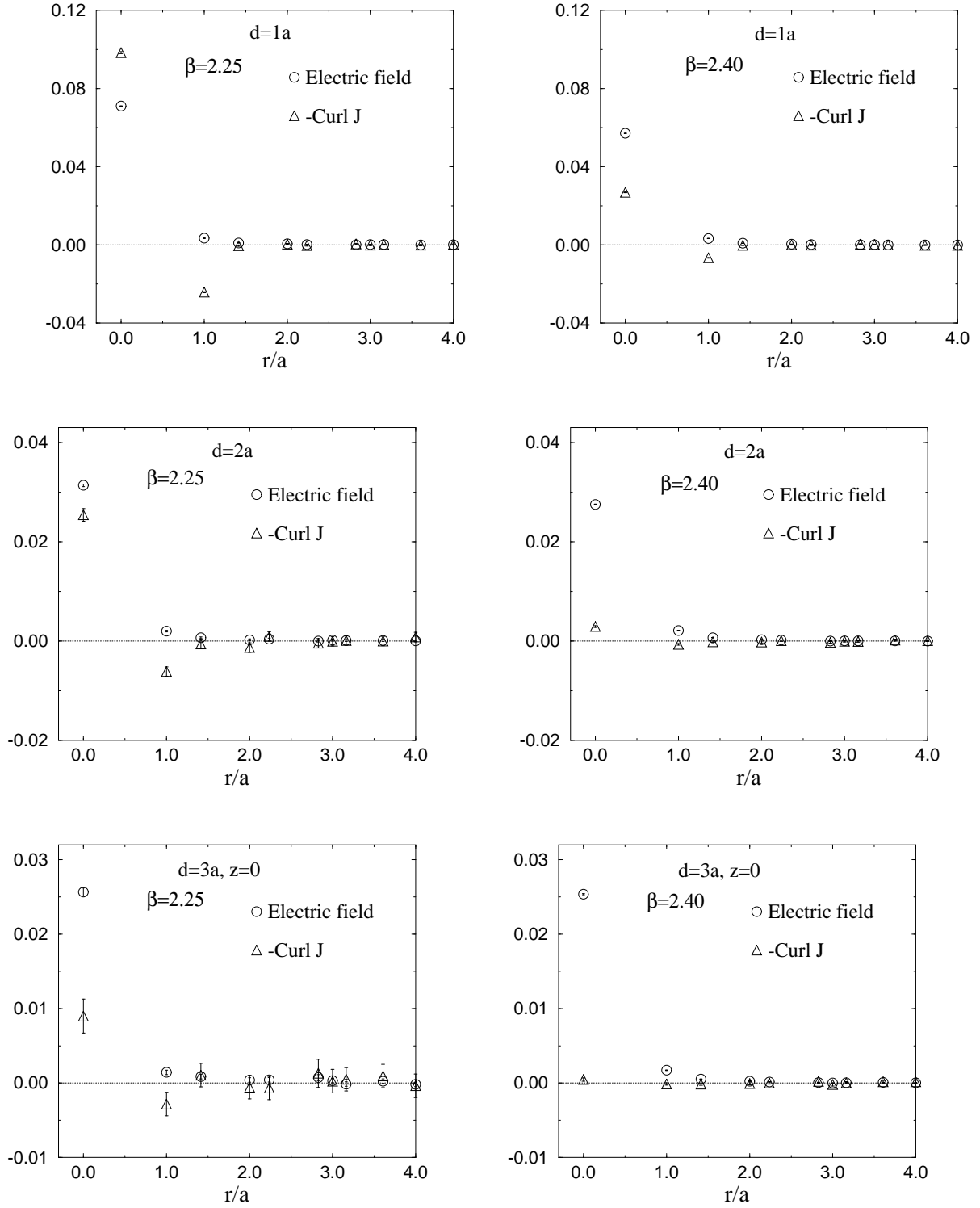


FIG. 6

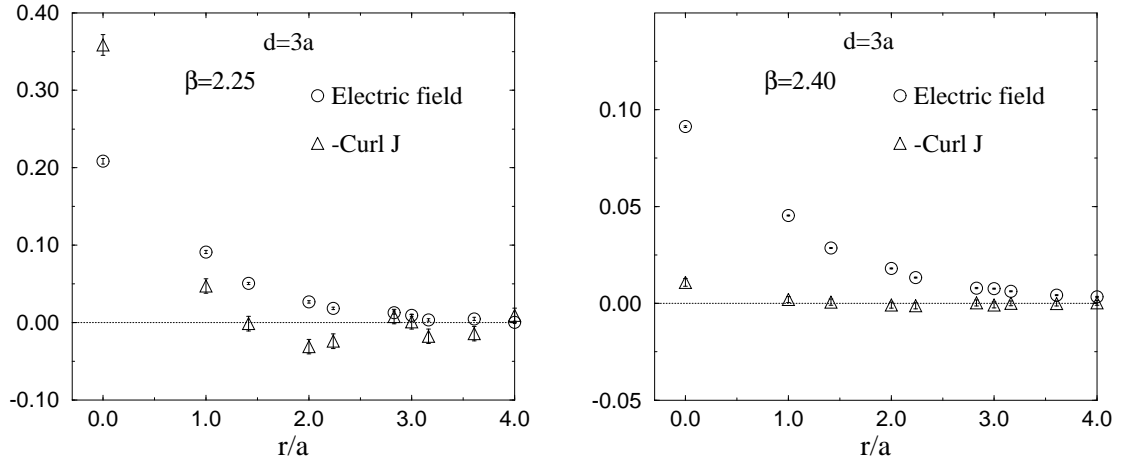


FIG. 7

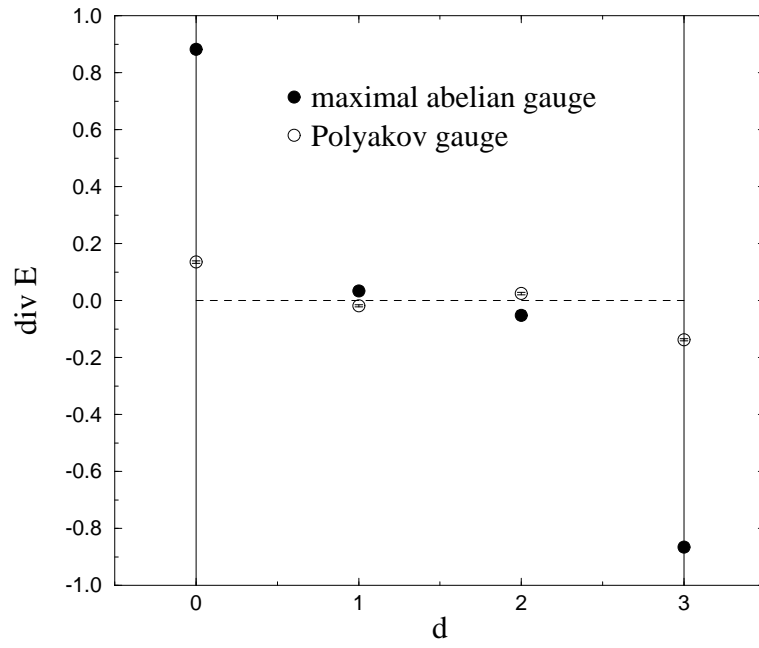


FIG. 8